Polymer Journal, Vol. 5, No. 1, pp 25—32 (1973)

Thermodynamic Studies of Solid Polyethers III. Poly(tetrahydrofuran), $-[-(CH_2)_4O-]_n-$

Shohei YOSHIDA,* Hiroshi SUGA, and Syûzô SEKI

Department of Chemistry, Faculty of Science, Osaka University, Toyonaka, Osaka, Japan.

(Received October 7, 1972)

ABSTRACT: A new type of DTA apparatus was constructed to detect glass transition and low temperature crystallization phenomena of Poly(tetrahydrofuran). Heat capacities were measured for two kinds of samples, annealed and rapidly cooled, in the temperature region between 11 and 330°K by using an adiabatic calorimeter. Thermal treatment effect was examined and the following thermodynamic values were determined: T_g=185 and 190°K and ΔC_p (at T_g)=19.4 and 15.8 $J°K^{-1}mol^{-1}$, for rapidly cooled and annealed samples respectively. For the completely crystalline state, T_m=314°K, ΔH_m= 12.4 $kJmol^{-1}$, and ΔS_m=39.3 $J°K^{-1}mol^{-1}$ were found. Further, heat capacities were analysed by using Tarasov's model. Glass transition temperatures of several polyethers were compared using our data and those from other workers.

KEY WORDS Poly(tetrahydrofuran) / Polyethers / DTA Apparatus / Heat Capacity / Low Temperature / Glass Transition / Melting / Tarasov's Model /

Poly(tetrahydrofuran) (abbreviated as PTHF) is a member of the polyether series $[-(CH_2)_mO-]_n$ with m=4. This substance has been investigated from various standpoints by several workers.

Tadokoro, *et al.*,[1,2] have investigated the structure of PTHF and analysed normal vibrations of its crystalline state, based on infrared and Raman spectra. According to their results, the crystal structure of PTHF is monoclinic: C_{2h}^6—C2/c, Z=2. Previous calorimetric study of PTHF is contained in a report by Melia, *et al.*[3] They have measured heat capacities of PTHF between 80 and 320°K. In their study the glass transition was found around 185°K; there was no report of low temperature crystallization.

In the present investigation, we intended to study thermal properties in the low temperature region below 80°K and to detect glass transition as well as low temperature crystallization phenomena.

As a preliminary experiment, the outline of thermal behavior was examined by use of an ordinary DTA apparatus and DSC (Perkin-Elmer Co.). The glass transition temperature (T_g) as well as a low-temperature crystallization effect had never been detected. These two phenomena, however, were clearly detected by using a novel type of DTA apparatus constructed in the present investigation. The behavior around T_g was also precisely measured by use of an adiabatic calorimeter.

Heat capacity was measured in the wide temperature region between 11 and 330°K by the precise adiabatic calorimeter for two samples crystallized under different conditions. Based on this result, the thermal treatment effect upon heat capacity was examined and heat capacity data were analysed by using Tarasov's model.[10] In addition, the changes in thermodynamic values on melting were evaluated.

Furthermore, we compared and examined glass transition temperatures of polyethers using our data and those reported in the literature.

EXPERIMENTAL

Preparation of PTHF

The monomer tetrahydrofuran (JIS-Special grade) (Nakarai Chemicals) was dried with sodi-

* Present address: Ashigara Research Laboratory, Fuji Photo Film, Co., Minamiashigara, Kanagawa.

um and then purified with repeated distillation. The monomer thus purified was polymerized with triethyl aluminum (Texas Alkyls), water, and epichlorohydrin (Nakarai Chemicals) as catalyst, after the method of Saegusa, *et al.*[4] The polymer thus synthesized was purified by precipitation from its tetrahydrofuran solution with water and then dried in vacuum (10^{-5} mmHg) at room temperature for three days. The average molecular weight was determined to be *ca.* 9×10^4 by measuring the viscosity, using the data of Kurata, *et al.*[5]

DTA Apparatus

In a preliminary experiment before the heat capacity measurements, a conventional DTA apparatus and/or DSC (model-1B) (Perkin-Elmer) was used. But we did not detect any glass transition phenomena. Thus, we constructed a special type of DTA apparatus for the detection of T_g.

In designing this apparatus, two points were specially taken into account: first, the fastest possible rate of cooling the sample from its molten state to the glassy state and, second, a high sensitivity of detection. In order to achieve these two conditions, we had to use only a small amount of sample. The schematic diagram for the construction of this apparatus is shown in Figure 1. It consists of a glass dewar vessel, a vacuum jacket, and a copper heater block attached to the sample pans. The constantan wire of the thermocouple for detection of differential temperature was soldered directly to these pans. For the temperature measurement of the sample a chromel-P—constantan thermocouple was employed.

Quenching to the glassy state was carried out as follows. First, the block equipped with the sample was heated up above the melting point of the sample. Then it was quickly wound down into the liq. N_2 in the dewar vessel by use of the pulley. The cooling rate by this procedure was at least $50°K\,sec^{-1}$. After this procedure was over, the liq. N_2 was evaporated up with a heater set at the bottom of the dewar vessel. Then the vacuum jacket and the dewar vessel were evacuated down to 10^{-5} mmHg. This apparatus worked properly for detection

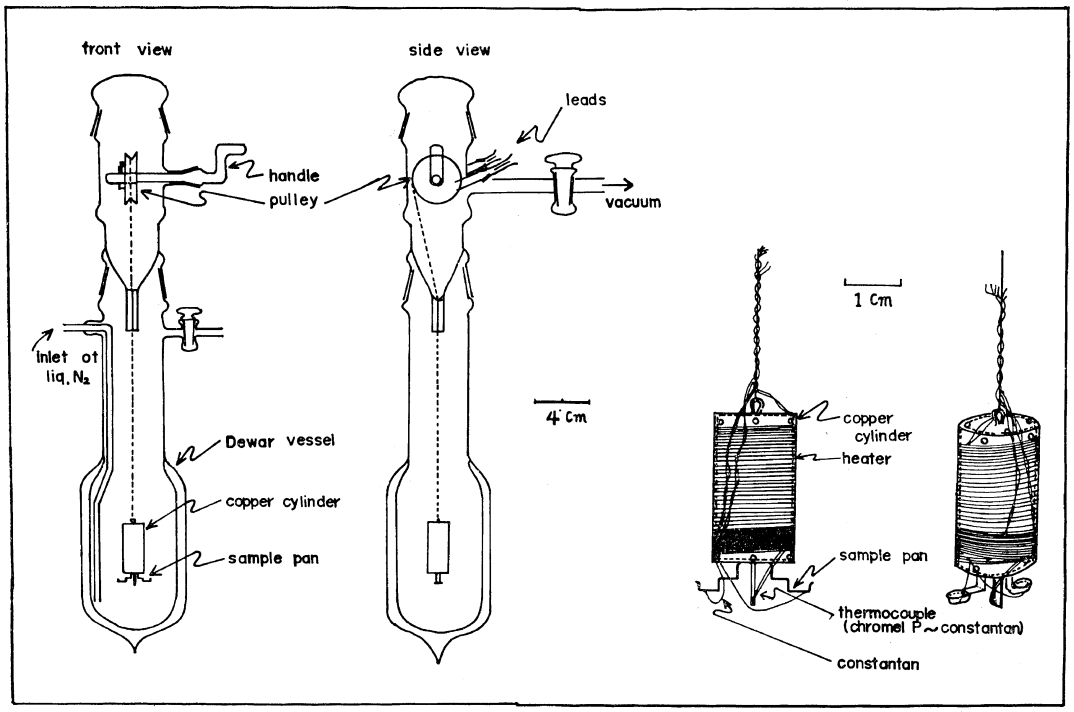

Figure 1. DTA apparatus designed for detection of glass transition.

of the existence of the glass transition, but the reproducibility was rather poor and the errors in temperature measurement amounted to $\pm 15°K$. Accordingly, this apparatus was used only for a supplementary experiment in this investigation.

Measurement of Heat Capacity

The apparatus used was an adiabatic calorimeter[6] designed for heat capacity measurement in the temperature region from 11 to 360°K. Platinum resistance thermometers manufactured by Leeds & Northrup Co. were used and these were calibrated by comparison with a platinum-resistance thermometer calibrated at the U.S. National Bureau of Standards. The sample container was made of copper, its capacity was about 20 cm^3.

The measurement of heat capacity was performed for two samples subjected to different thermal treatments in the temperature region from 11 to 330°K. One of these was an annealed sample which was chilled from 320 to 270°K at the rate of 1°K/hr, heated up again to 290°K and then held in the temperature range 290—305°K for 40 hr. Another sample was prepared by cooling the melt down to liq. N_2 temperature at the rate of 18°K/min. These thermal treatments were carried out in the calorimeter cell. The heat capacity was measured by means of the intermittent heating technique, but at the melting process the continuous heating technique was employed. The heating rate during the measurement was 3 to 7°K/hr.

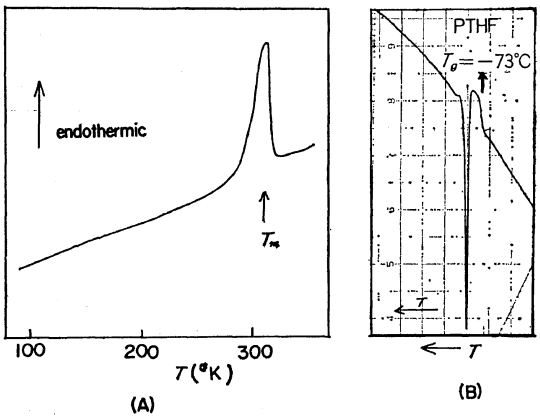

Figure 2. DTA curves of PTHF: (A), by conventional DTA apparatus; (B), by special DTA apparatus.

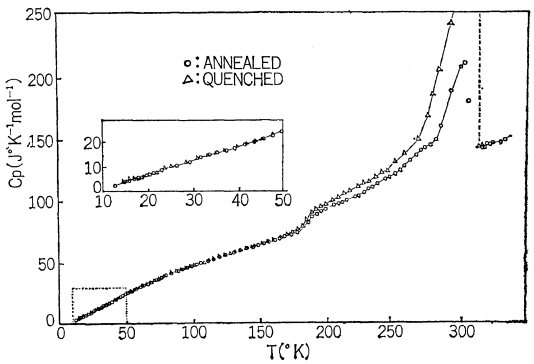

Figure 3. Heat capacity of PTHF (○, annealed; △, rapidly cooled).

RESULTS AND DISCUSSIONS

Heat-Capacity Data

The DTA curve obtained by use of conventional equipment is shown in Figure 2 (A); the melting temperature was found to be near 313°K, but the glass transition and low temperature crystallization phenomena were not detected. These two phenomena, however, were clearly detected by using the special type of DTA apparatus described in the preceding section. The weight of the sample used in this measurement was only about 1 mg. The original chart thus obtained is shown in Figure 2 (B).

The heat capacity is shown in Figures 3 and 4 and listed in Tables I and II. T_g was found

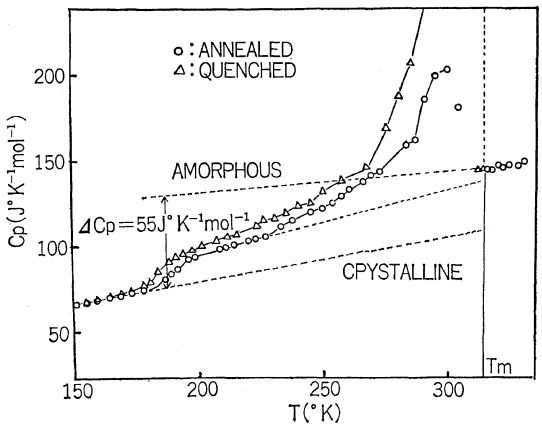

Figure 4. Heat capacity of PTHF: ○, annealed; △, rapidly cooled.

Table I. Heat capacity of PTHF (annealed)

T/K	C_p/JK^{-1}mol^{-1}	T/K	C_p/JK^{-1}mol^{-1}
12.68	2.105	130.62	57.87
14.74	3.656	135.22	59.36
15.86	4.168	139.69	60.80
16.85	4.781	144.01	61.95
17.77	5.365	148.26	63.66
19.60	6.439	152.42	64.98
20.47	6.713	156.46	66.33
21.80	7.528	164.32	69.11
23.80	8.602	168.63	70.80
26.46	10.30	173.33	72.36
29.21	11.76	177.96	74.29
31.52	13.33	185.29	82.56
33.56	14.66	188.70	87.05
35.46	15.62	192.07	89.18
37.41	16.53	195.44	91.79
39.49	17.75	198.74	93.13
41.66	19.07	208.34	97.96
43.79	20·38	211.44	98.66
45.85	21.54	213.89	101.8
47.85	22.68	220.18	103.9
49.83	23.85	223.53	104.3
51.90	25.35	226.57	105.0
54.04	26.21	233.74	111.6
56.19	27.58	237.77	114.0
58.35	28.65	245.98	119.6
60.55	29.95	250.01	122.1
62.78	39.10	254.00	124.8
65.01	32.19	257.92	128.5
67.19	33.10	261.77	133.3
69.46	34.24	265.57	137.3
71.80	35.25	269.30	141.1
74.07	36.00	272.96	143.1
76.26	37.31	284.00	160.1
79.40	39.53	287.74	161.3
83.44	41.05	291.29	188.9
87.31	42.79	294.68	198.6
91.04	44.10	298.03	201.5
94.67	45.29	304.68	180.7
98.19	46.55	316.84	143.2
101.75	47.81	318.33	146.3
105.70	49.27	320.18	145.7
110.16	50.96	322.39	147.2
114.75	52.54	324.97	146.5
119.22	54.09	328.97	147.4
123.59	55.53	331.73	149.4
125.55	56.34		

Table II. Heat capacity of PTHF (rapidly cooled)

T/K	C_p/JK^{-1}mol^{-1}	T/K	C_p/JK^{-1}mol^{-1}
14.57	3.619	135.14	59.47
15.05	3.800	139.21	60.79
15.78	4.197	143.21	62.23
17.66	4.961	147.16	63.71
18.81	5.949	151.17	65.21
20.00	6.728	155.49	66.88
21.51	6.014	159.81	68.55
25.91	10.27	165.08	70.28
28.61	11.81	169.80	72.04
31.06	13.51	173.86	73.74
33.22	13.73	177.95	76.67
35.30	15.76	181.51	79.14
37.48	17.08	184.99	84.58
39.72	18.24	188.37	90.58
41.88	19.51	191.67	93.18
43.87	20.63	194.98	95.17
45.78	21.46	198.28	97.24
51.52	25.12	201.38	99.11
53.57	26.14	207.66	103.4
59.96	29.30	211.71	105.7
62.13	30.67	216.89	108.3
64.29	31.68	223.88	112.1
68.51	33.79	227.64	114.7
70.58	34.71	231.38	115.7
72.66	35.61	235.49	119.5
74.71	36.49	240.28	123.5
76.77	37.91	245.26	124.7
78.80	38.43	250.17	132.0
83.88	41.23	257.63	138.8
87.28	41.98	267.83	151.1
90.98	43.99	275.52	169.3
94.33	44.90	280.63	187.3
97.55	46.21	285.54	206.5
100.69	47.35	290.29	244.0
107.14	49.70	294.95	310.5
110.89	51.15	299.40	428.6
114.69	53.26	303.60	706.1
119.84	54.62	312.79	144.7
123.51	55.67	315.37	144.9
127.41	56.84	318.79	145.6
130.98	58.18	323.05	148.1

around 185°K and was not followed by a crystallization effect, irrespective of the thermal histories. This is consistent with the general behavior of a semicrystalline polymer containing a small amorphous part: no matter how this amophous part shows the glass transition, it does not show any crystallization phenomenon. The premelting started around 230°K and the

melting finished at 314°K, which is defined as the melting temperature of the sample.

The heat capacities of the completely crystalline sample and the base line used in the evaluation of the enthalpy of fusion were estimated in the same way as in the previous work.[7] The heat capacities of the super-cooled liquid (completely amorphous state) were estimated by extrapolating those of the liquid to the glass transition temperature. To minimize the ambiguity of this extrapolation, Wunderlich's suggestion[8] for the heat capacity at the glass transition temperature was taken into account. Comparing these heat capacity values with each other, the crystallinity was evaluated to be about 70 and 65% for the annealed and rapidly cooled samples respectively. The heat of fusion was then evaluated to be 8.68 kJ mol^{-1} for the annealed sample with 70-% crystallinity. By using these values, the heat of fusion of the completely crystalline sample was estimated to be 12.4 kJ mol^{-1} and the entropy of fusion was found to be 39.3 J°K^{-1} mol^{-1} (Conventionally, we evaluated this value by dividing ΔH_m by T_m (=314°K).

Below the glass transition region, the heat capacities of the rapidly cooled sample show almost the same values as those of the annealed one. In the low temperature region (below 25°K), the former are slightly larger than the latter but the difference between them is quite small. In general, the heat capacity of the glassy state is larger than that of the crystalline state. In this investigation, the crystallinities of both samples were different by only about 5% from each other. Thus, this difference did not affect the heat capacities within the experimental error. The effect might be, however, detectable in the helium temperature region. As a matter of fact, this type of difference was found for POCB.[9]

Analysis of Heat Capacity

Infrared and Raman spectra of PTHF were measured by Tadokoro, *et al.*[2] They analysed the normal vibration of the single chain of PTHF, using their data. The normal vibrations of PTHF were analysed under the factor group isomorphous to D_{2h} and calculated for the infrared active species of B_{1u}, B_{2u} and B_{3u}. In order to estimate roughly the dispersion of the normal vibrations, all the frequency values were plotted separately for two extreme cases of δ (=phase difference)=0 and $\delta=\pi$ (see Figure 5). In this case, it was taken into consideration that B_{3u} was optically active at $\delta=0$ and B_{1u} and B_{2u} were optically active at $\delta=\pi$.

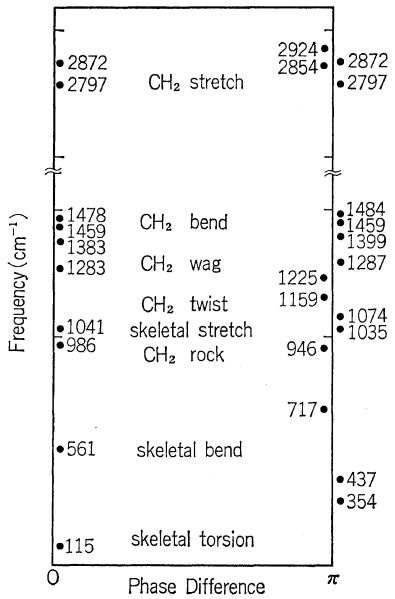

Figure 5. Normal vibrations of PTHF.

The number of normal vibrational modes of PTHF is 39 per chemical repeating unit; these are roughly classified into the CH_2 stretching, bending, wagging, twisting, and rocking modes and the skeletal stretching, bending, and torsional modes. These vibrational modes would have a frequency distribution, but the progression of the frequency within each distribution was unknown. Since the CH_2 stretching modes have very high frequencies, they will give rise to narrow distributions. The CH_2 bending, wagging, twisting, and rocking modes will be situated in the regions from 1478 to 1459 cm^{-1}, from 1399 to 1283 cm^{-1}, from 1225 to 1159 cm^{-1}, and from 946 to 717 cm^{-1}, respectively. The skeletal stretching vibrational modes will be situated in the region from 1074 to 986 cm^{-1}. The skeletal bending and torsional modes, which have lower frequencies than the modes mentioned above, will show very widely extended

Table III. Vibrations of PTHF

Vibrational mode	Average frequency, ν/cm^{-1}	Characteristic temperature, θ_E/K	Number of modes
CH_2 asym stretch.	2889	4157	4
CH_2 sym stretch.	2834	4078	4
CH_2 bend.	1473	2120	4
CH_2 wag.	1338	1925	4
CH_2 twist.	1192	1715	4
Skeletal stretch.	1034	1488	5
CH_2 rock.	946	1361	2
CH_2 rock.	717	1032	2
Skeletal bend.	561	807	1
Other modes	Tarasov's spectr		9
			39

distributions of frequencies.

The average frequencies of these vibrational modes and their characteristic temperatures, θ_E, are given in Table III. For the CH_2 rocking modes, two average frequencies and characteristic temperatures are given, since the frequencies of these modes extend over a rather wide frequency region. For the skeletal vibration modes, except the skeletal stretching one, only the maximum frequency of the skeletal bending mode and its characteristic temperature are given in this table for reference.

For the sake of theoretical considerations, the heat capacities of the completely crystalline state are necessary. Therefore, the experimental heat capacities of the annealed sample were corrected tentatively by use of the relationship between the crystallinity and the heat capacity found for POCB.[9] These corrections were found to be about 14, 6, and 3% at 15, 20, and 30°K, respectively. Thus, it should be negligible above 50°K. Further, the conversion of the observed heat capacities into ones at constant volume and the calculation of the heat capacity based on spectroscopic data were carried out by the same procedures as those used for POCB.[9]

The first case, where we tried to fit the contribution of all the skeletal vibrations into Tarasov's heat capacity,[10] was unsuccessful as in the case of POCB.[9] This was due to the fact that the skeletal stretching modes have very high frequencies in comparison with the other skeletal vibrational ones.

In the second case, the contribution of the

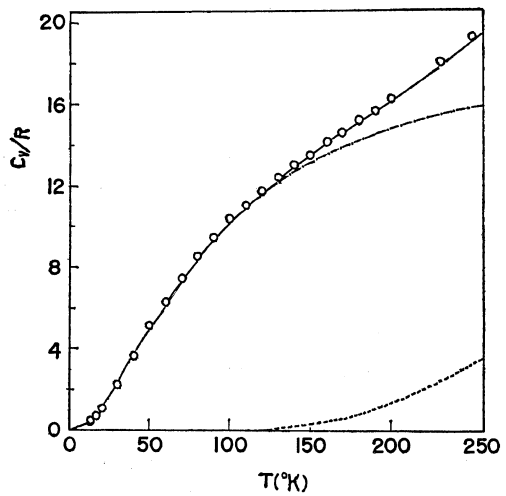

Figure 6. Heat capacity of PTHF: ○, exptl; ——, calcd (total); – – –, Tarasov approximation; ------, by skeletal stretch. and CH_2 group vibrations.

CH_2 groups and skeletal stretching vibrations was approximated by the Einstein model and then the remaining other vibrations by Tarasov's model.[10] This met with a fair amount of success. The calculated heat capacity data are shown in Figure 6 and given in Table IV, together with the experimental heat capacity. In this case, θ_1, θ_3 and θ_3/θ_1 were evaluated to be 550°K, 103°K and 0.187, respectively. Based on these results, the heat capacity of PTHF is successfully reproduced by the relation:

$$C_v = 10RC_{1,3}(\theta_1, \theta_3) + 5RE(\theta_E^s) + R\sum^{24} E(\theta_E)\ ,$$

(per mole of repeating unit)

Table IV. Experimental and calculated heat capacities of PTHF

	C_v/R per mole of repeating unit		
T/K	Experimental	Calculated	Deviation, %
15	0.387	0.392	+1.3
20	0.748	0.742	−0.8
30	1.439	1.478	+2.7
40	2.130	2.180	+2.3
50	2.855	2.839	−0.7
60	3.520	3.469	−1.4
70	4.120	4.066	−1.4
80	4.653	4.626	−0.6
90	5.148	5.148	0
100	5.597	5.625	+0.5
110	5.997	6.060	+1.1
120	6.387	6.461	+1.2
130	6.758	6.824	+1.0
140	7.103	7.152	+0.7
150	7.434	7.482	+0.7
160	7.751	7.783	+0.4
170	8.067	8.080	+0.2
180	8.366	8.365	0
190	8.653	8.663	+0.1
200	9.025	8.946	−0.9
230	9.921	9.843	−0.8
250	10.50	10.47	−0.8

where $C_{1,3}$ is Taraspv's heat capacity function with $\theta_1=550$°K and $\theta_3=103$°K and E the Einstein function with θ_E^S and θ_E for the characteristic temperatures of the skeletal stretching and CH_2 group vibrations, respectively.

In the third trial, the contribution of the one special bending mode was additionally treated by the Einstein function and the remainder was approximated by Tarasov's model. In this case, θ_1, and θ_3 were evaluated to be 500 and 106°K, respectively. Comparing the result of this case with that of the second one, the latter seems to be better than the former.

Finally, it may be noted again that the calculated heat capacities in the low temperature region (below 30°K) and above the glass transition region will contain an ambiguity to some extent, since the heat capacity data in these two regions were the corrected values for the 100-% crystallinity and/or the extrapolated values from lower temperatures.

Glass Transition Temperatures of Polyethers

In the series of polyethers, POCB is found to attain the glassy state by rapid cooling.[7] But, for other polyethers, it is rather difficult to form the completely glassy state. However, in our investigation, the glass transition temperatures of the semicrystalline sample of PTHF and POMO[11] were found by precise heat capacity measurement. The glass transition temperatures thus obtained are shown in Figure 7, together with those for POM, PEO, and PE, which were found by other investigators. The data for POM is taken from the work by Dainton, *et al.*,[12] and Swallow, *et al.*[13] The glass transition of PE has been investigated by numerous workers but their data are inconsistent with each other. In this figure data by Mandelkern,[14] Miller,[15] and Wyman[16] are adopted.

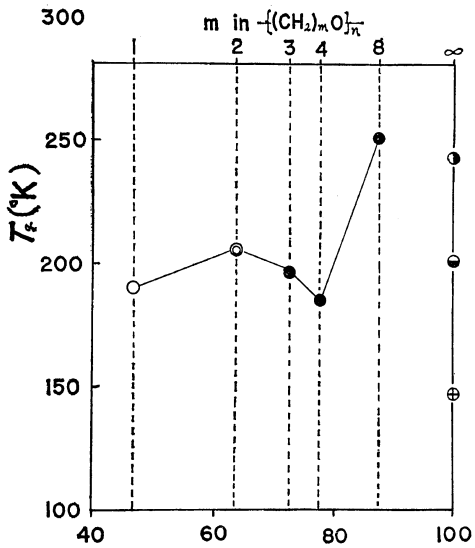

Figure 7. Glass transition temperature of polyethers: ●, present work; ○, by Dainton; ◎, by Swallow; ⊕, by Mandelkern; ◒, by Miller; ◑, by Wyman.

As is shown in this figure, the glass transition temperatures do not show any systematic change such as that shown by the melting temperatures Faucher, *et al.*,[17] examined the glass transition temperatures of polyethers by viscoelastic measurement and concluded that the glass transition temperatures changed linearly with the change of the methylene content of polyethers. However, in their investigation, the assignment of the glass transition temperature in viscoelastic constant *vs.* temperature curve seems to be am-

biguous, since they did not distinguish the absorption peaks due to the glass transition from other peaks caused by other origins.

Acknowledgment. The authors wish to express their sincere thanks to Professor H. Tadokoro, Assistant Professor Y. Chatani, and Dr. M. Kobayashi of Osaka University for the detailed information about the structural and spectroscopic data for PTHF. Thanks are due to Professor H. Fujita of Osaka University and Dr. K. Nakao of Industrial Research Institute, Osaka Prefecture, for allowing the authors to use the apparatus for molecular weight measurement and the gel-permeation chromatography apparatus respectively.

REFERENCES

1. K. Imada, T. Miyakawa, Y. Chatani, and H. Tadokoro, *Makromol. Chem.*, **83**, 113 (1965).
2. K. Imada, H. Tadokoro, A. Umehara, and S. Murahashi, *J. Chem. Phys.*, **4**, 2807 (1965).
3. G. A. Clegg, D. R. Gee, T. P. Melia, and A. Tyson, *Polymer*, **9**, 501 (1968).
4. T. Saegusa, H. Imai, and J. Furukawa, *Makromol. Chem.*, **65**, 60 (1963).
5. M. Kurata, H. Uchiyama, and K. Kamada, *ibid.*, **88**, 281 (1965).
6. T. Matsuo, H. Suga, and S. Seki, *J. Phys. Soc. Jap.* **30**, 785 (1971).
7. S. Yoshida, M. Sakiyama, and S. Seki, *Polymer J.*, **1**, 573 (1970).
8. B. Wunderlich, *J. Phys. Chem.*, **64**, 1052 (1960).
9. S. Yoshida, H. Suga, and S. Seki, *This Journal, to be publiched.*
10. V. V. Tarasov, "*New Problems in the Physics of Glass*," *Israel Program for Scientific Translations, Jerusalem*, (1963).
11. S. Yoshida, H. Suga, and S. Seki, *Polymer J.*, **5**, 000 (1973).
12. T. P. Melia, F. S. Dainton, D. M. Evans, and F. E. Hoare, *Polymer*, **3**, 263 (1962).
13. J. C. Swallow and D. J. Marks, *Ph. D. Thesis, Manchester*, (1961).
14. F. C. Stehling and L. Mandelkern, *Macromolecules*, **3**, 242 (1970).
15. A. A. Miller, *J. Polymer Sci., Part A-2*, **6**, 249 (1968).
16. J. H. Magill, S. S. Pollack, and D. D. Wyman, *ibid., Part A*, **3**, 3781 (1965).
17. J. A. Faucher and J. V. Koleske, *Polymer*, **9**, 44 (1968).